BUTTERWORTH HEINEMANN

Polymer Vol. 36 No. 26, pp. 4927–4933, 1995

0032-3861/95/$10.00+0.00

Mass spectral characterization of the thermal degradation of poly(propylene oxide) by electrospray and matrix-assisted laser desorption ionization

Zachary Barton, Terence J Kemp*, Armelle Buzy and Keith R. Jennings
Department of Chemistry, University of Warwick, Coventry CV4 7AL, UK
(Received 23 May 1995; revised 7 July 1995)

The thermal degradation of poly(propylene oxide) (PPO), $M_n = 2000$, can be characterized by electrospray (ESI) and matrix-assisted laser desorption ionization (MALDI). ESI and MALDI spectra of partially degraded PPO provide strong support for the thermal degradation pathway previously suggested by Griffiths *et al.* and Lemaire *et al.* Although these pathways differ in detail, it is not possible to distinguish between them from the masses of the resultant degradation species. Gel permeation chromatography data indicate that both mass spectrometric methods emphasize the presence of low-mass material, particularly in the degraded samples. This is attributed to the different sensitivities of the two techniques and some *in situ* fragmentation during mass spectrometric analysis.

(Keywords: poly(propylene oxide); electrospray; laser desorption)

INTRODUCTION

Poly(ethylene glycol)s (PEGs) have been well characterized by electrospray (ESI)[1] and matrix-assisted laser desorption ionization (MALDI)[2] mass spectrometry. Poly(propylene oxide) (PPO) is well characterized by MALDI[2] but not nearly so well by ESI. ESI[3] and MALDI have been used successfully to determine relative molecular masses (*RMM*s) and structural information from a wide range of biomolecules such as peptides[4], proteins[5] and oligonucleotides[5]. In view of the importance of PPO in polyurethane elastomers and foams[6] which undergo rapid oxidative degradation at elevated temperatures, we have sought to apply ESI and MALDI to the characterization of the degradation pathways and products. The thermal degradation of PPO has been studied by gas phase infra-red and ^{1}H nuclear magnetic resonance (n.m.r.) spectroscopic measurements by Griffiths *et al.*[6] and the photodegradation has been studied using solution infrared by Lemaire *et al.*[7] Mechanistic schemes based on hydroperoxide formation have been put forward for the oxidation processes. This paper substantiates a hydroperoxide mechanism but shows that the scheme proposed by Lemaire *et al.*[7] giving oxidation predominantly at the secondary carbon better explains the relative product abundances observed by ESI and MALDI as compared to oxidation predominantly at the tertiary carbon proposed by Griffiths *et al.*[6]. This paper also provides a comparison of the application of gel permeation chromatography (g.p.c.), MALDI and ESI to the characterization of the thermal degradation products of a well-known polymer.

* To whom correspondence should be addressed

EXPERIMENTAL

Materials

Linear PPO, $H[OCH(CH_3)CH_2]_nOH$ was obtained from ICI. The nominal *RMM* was 2000.

ESI mass spectrometry

The ESI experiments were carried out in a Fisons' 'Quattro II' triple quadrupole mass spectrometer (VG Biotech, Altrincham, UK) equipped with an atmospheric pressure ionization (API) source operated in the nebulizer-assisted electrospray mode. The potential on the electrospray needle was set at 3.5 kV and the extraction cone voltage was varied between 20 and 80 V. PPO at a concentration of 0.5 μg μl^{-1} was dissolved in a mixture of tetrahydrofuran (THF) and methanol (1 : 1 by volume) in the presence of 0.5% ammonium chloride. Aliquots of 20 μl were introduced into the ion source at a flow rate of 5 μl min^{-1}. Mass spectra were acquired over the m/z range 3000–350 during a 10 s scan, and, by operating the data system in the multichannel acquisition (MCA) mode, 30 scans were summed to produce the final spectrum. Calibration was carried out using a solution of sodium iodide.

MALDI mass spectrometry

The MALDI experiments were carried out on a Kratos Kompact III spectrometer. The instrument was fitted with a nitrogen laser of wavelength 337 nm and was operated in the linear mode. Sample concentrations were approximately 10^{-4} M in a mixture of methanol and water (1 : 1) in the presence of 0.5% sodium chloride. Matrix (2,5-dihydroxybenzoic acid) concentrations were approximately 10^{-1} M. Equal volumes of matrix and

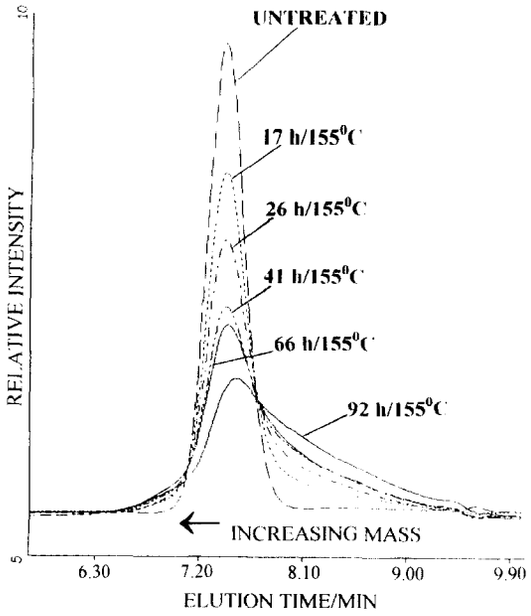

Figure 1 Gel permeation chromatograms of untreated and pyrolysed PPO obtained using THF as the solvent

Table 1 *RRM* of the thermal degradation products of PPO

Fragment	C	E	F	G
RMM	$2+(58n)$	$46+(58n)$	$16+(58n)$	$18+(58n)$

analyte solutions were mixed and 1–2 μl placed on a target slide and air dried. Every sample was analysed at various laser powers and spectra were averaged over 100 shots.

G.p.c.

Molecular weight data were obtained using a Polymer Laboratories' modular GPC system equipped with one 15 cm Plgel 3 μm mixed-E-column and calibrated using Polymer Laboratories' narrow PPO standards. The solvent was THF, delivered at 1 ml min^{-1}.

Thermal degradation

PPO (1 g) was placed in a glass vial (10 ml). Heating was carried out in a Gallenkamp oven at 155°C. Samples (0.05 g) were removed after 17, 26, 41, 66 and 92 h.

RESULTS AND DISCUSSION

G.p.c.

Figure 1 shows the gel permeation chromatograms for untreated and pyrolysed PPO. It is clear from *Figure 1* that chain scission is the predominant thermal degradation mechanism at 155°C leading to a reduction in the M_n. A small amount of cross-linked material is however apparent below 7.0 min in the chromatogram.

Thermal degradation mechanisms

Two possible mechanisms operating in parallel have been proposed by Griffiths *et al.*[6] based on hydroperoxide formation at both the secondary and tertiary

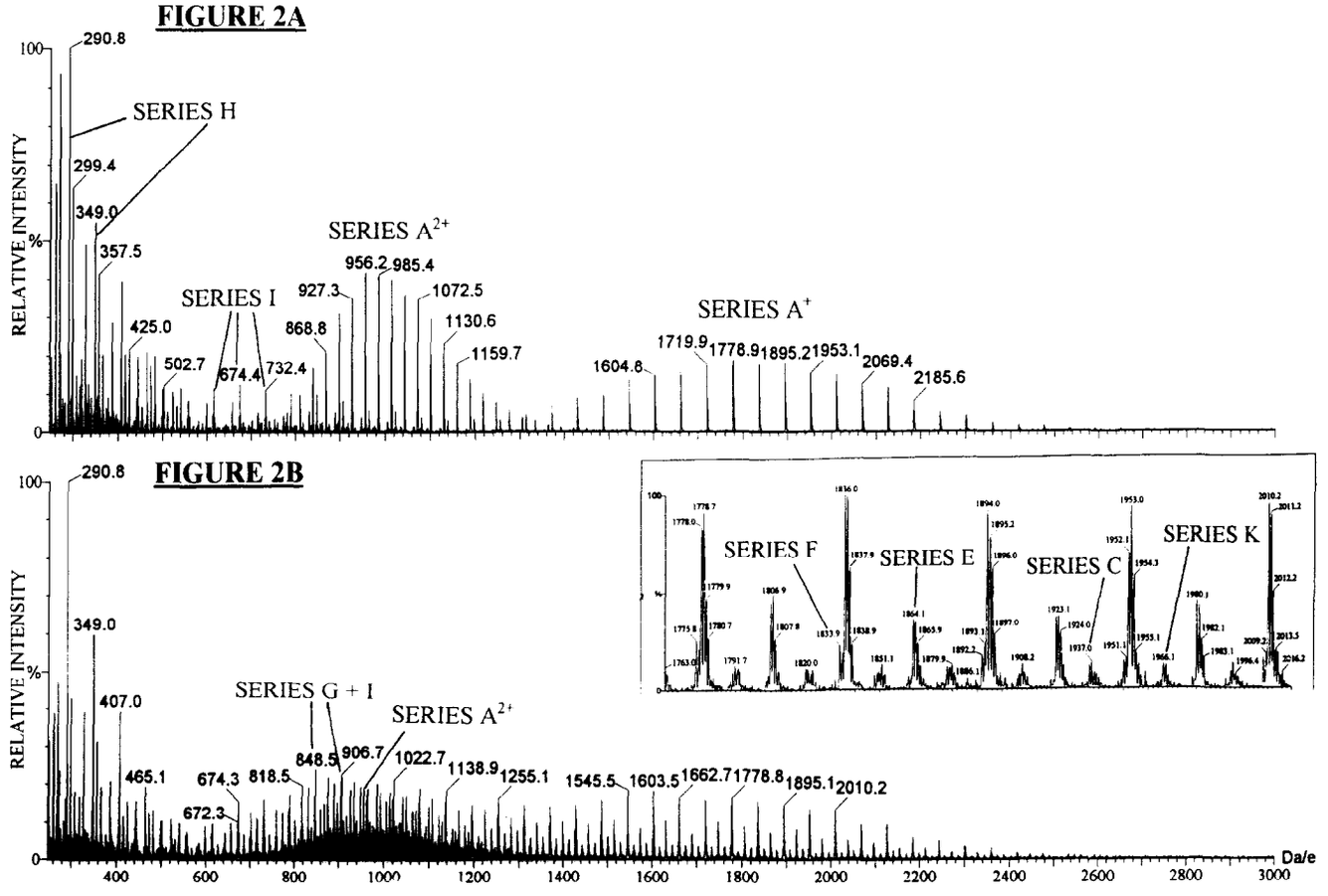

Figure 2 Electrospray mass spectrum of (A) untreated PPO and (B) pyrolysed PPO; mobile phase THF/MeOH (50/50) containing 0.5% aqueous NH_4Cl. Assignments of ions are given in *Table 2*

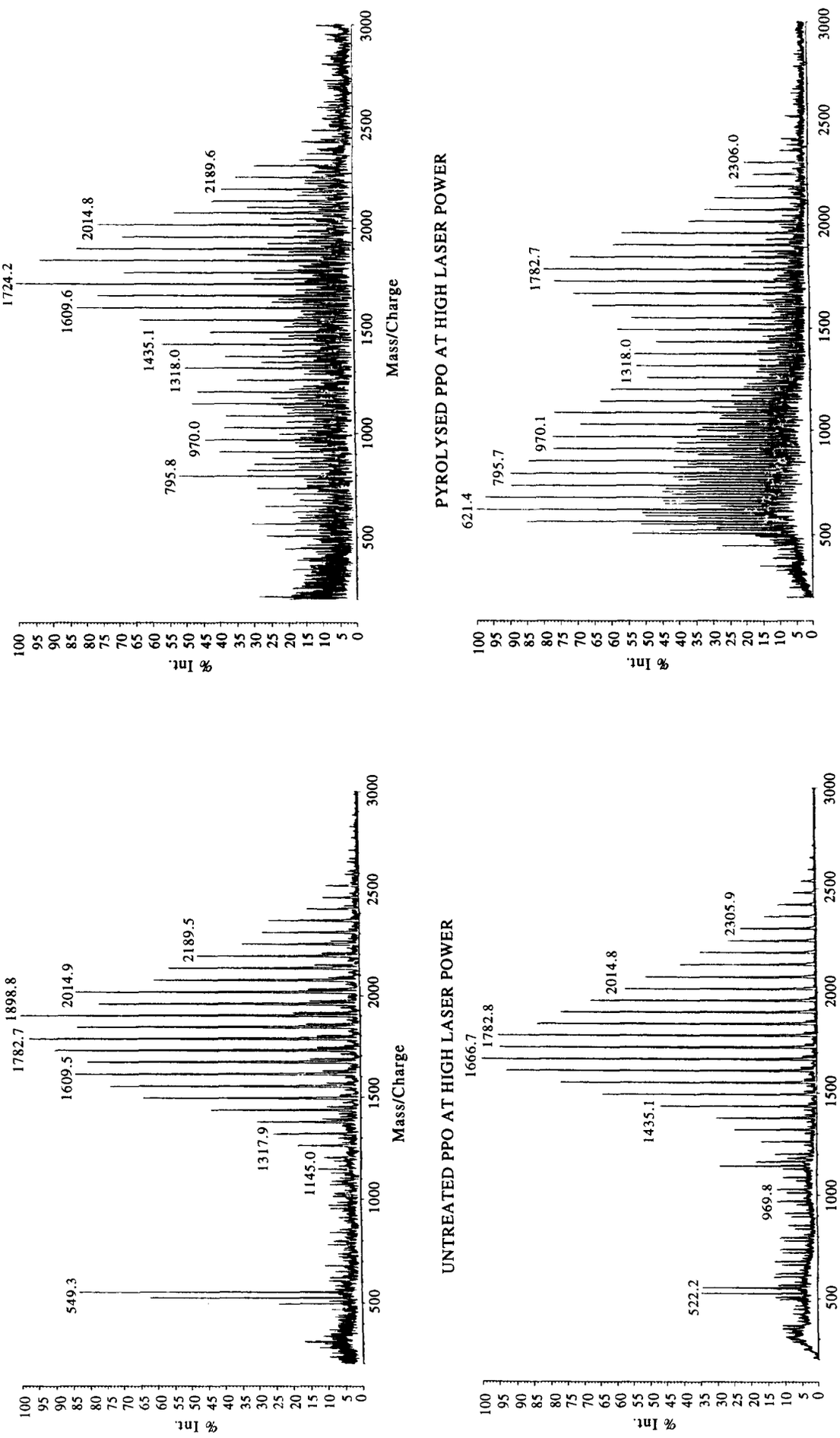

Figure 3 Matrix-assisted laser desorption ionization spectra of untreated and pyrolysed PPO. Sample concentrations were approximately 10^{-4} M in a mixture of methanol and water (1 : 1) in the presence of 0.5% sodium chloride. Matrix (2,5-dihydroxybenzoic acid) concentrations were approximately 10^{-1} M

Table 2 Assignments of principal peaks in the ESI spectrum of degraded PPO

Series A^{+}
$HO-[CH_2-CH(CH_3)-O]_nH.NH_4^+$

n	m/z
26	1545.5
27	1603.5
28	1661.8
29	1719.7
30	1778.0
31	1836.1
32	1894.0
33	1952.2
34	2010.2
35	2068.4

Series A^{2+}
$HO-[CH_2-CH(CH_3)-O]_nH.(NH_4^+)_2$

n	m/z
26	781.6
27	810.7
28	839.7
29	868.7
30	897.8
31	927.3
32	956.2
33	985.4
34	1014.3
35	1043.2

Series C and C′
C: $(CH_3)C(O)-O-[CH_2-CH(CH_3)-O]_nH.NH_4^+$
C′: $HC(O)-CH_2[O-CH(CH_3)CH_2]_{n-1}$

n	m/z
26	1588.7
27	1645.7
28	1703.9
29	1762.8
30	1820.0
31	1878.0
32	1936.0
33	1994.2
34	2052.3
35	2111.4

Series E and E′
E: $HO-[CH_2-CH(CH_3)-O]_x-C(O)H.NH_4^+$
E′: $CH(CH_3)O-[CH_2-CH(CH_3)-O]_yH.NH_4^+$

n	m/z
26	1573.9
27	1632.0
28	1690.0
29	1748.0
30	1806.0
31	1864.1
32	1922.1
33	1980.1
34	2038.1
35	2096.2

Series F and F′
F: $HO-[CH_2-CH(CH_3)-O]_x-CH_2-C(O)CH_3.NH_4^+$
F′: $H(O)C-CH(CH_3)-O-[CH_2-CH(CH_3)-O]_yH.NH_4^+$

n	m/z
26	1601.7
27	1659.7
28	1717.8
29	1775.8
30	1833.9
31	1892.2
32	1950.2
33	2008.3
34	2066.3
35	2124.3

Series G
$HO-[CH_2-CH(CH_3)-O]_yH.NH_4^+$

n	m/z
26	1545.7
27	1603.7
28	1661.7
29	1719.9
30	1778.0
31	1836.0
32	1894.0
33	1952.1
34	2010.2
35	2068.4

Series H
$HO-[CH_2-CH(CH_3)-O]_x-CH_2-CH(CH_3)$

n	m/z
4	290.8
5	349.0
6	407.0
7	465.2
8	523.1
9	581.3
10	

Series I
$HO-[CH_2-CH(CH_3)-O]_xH.NH_4^+$

n	m/z
4	
5	
6	383.9
7	442.1
8	500.1
9	558.1
10	616.3
11	674.3
12	732.4
13	790.5
14	848.5
15	906.5
16	964.6
17	1022.7

Series J
$HO-[CH_2-CH(CH_3)-O]_yH.H^+$

n	m/z
4	250.9
5	308.9
6	366.9
7	425.1
8	483.1
9	541.2
10	599.4
11	657.2
12	
13	
14	
15	
16	
17	

Table 2 (Continued)

Series K

$HO-[CH_2-CH(CH_3)-O]_x-C(O)-CH(CH_3)-O-[CH_2-CH(CH_3)-O]_y H.NH_4^+$

m/z
1617.8
1675.9
1733.9
1791.9
1850.0
1908.0
1966.0
2024.0
2082.1

carbon atoms. These authors favour the tertiary hydroperoxide mechanism as follows:

$$HO-[CH_2-CH(CH_3)-O]_x-CH_2-C(CH_3)(OOH)-O-[CH_2-CH(CH_3)-O]_y H$$
$$\downarrow$$
$$HO-[CH_2-CH(CH_3)-O]_x-CH_2-C(CH_3)(O\cdot)-O-[CH_2-CH(CH_3)-O]_y H$$
$$HO\cdot + RH \rightarrow H_2O + R\cdot$$

Here RH is a polymer molecule and the R· radical leads to more hydroperoxide formation.

Pathway 1. C–C bond cleavage adjacent to the alkoxy centre takes place to generate products **B** and **C**, followed by further peroxidxation of product **B**:

$$\underset{\textbf{(B)}}{HO-[CH_2-CH(CH_3)-O]_x-CH_2\cdot} \quad \underset{\textbf{(C)}}{(CH_3)C(O)-O-[CH_2-CH(CH_3)-O]_y H}$$
$$\text{i)} + O_2 \downarrow \text{ii)} + RH$$
$$\underset{\textbf{(D)}}{HO-[CH_2-CH(CH_3)-O]_x-CH_2OOH} \rightarrow \underset{\textbf{(E)}}{HO-[CH_2-CH(CH_3)-O]_x-C(O)H}$$
$$+R\cdot \qquad\qquad + H_2O$$

Pathway 2. C–O bond cleavage adjacent to the alkoxy group takes place to generate products **F** and **G**:

$$\underset{\textbf{(F)}}{HO-[CH_2-CH(CH_3)-O]_x-CH_2-C(O)CH_3} \quad \cdot O-[CH_2-CH(CH_3)-O]_y H$$
$$\text{i)} + RH \downarrow$$
$$\underset{\textbf{(G)}}{HO-[CH_2-CH(CH_3)-O]_y H}$$
$$+R\cdot$$

Griffiths *et al.*[6] note that these two processes taken together give the observed acetate, formate and ketone end groups, but the acetate and formate are produced in equal amounts instead of the 2 : 3 ratio as found by n.m.r. However, more formate could result from breakdown of the less readily formed secondary hydroperoxide.

Table 1 gives the expected *RMM* of the species resulting from these two pathways, namely C, E, F and G [the original PPO molecule has an *RMM* of $18 + (58n)$].

The mechanism of oxidation at the secondary carbon atom proposed by Lemaire *et al.*[7] is shown below. As with the oxidation at the tertiary carbon atom, two processes operating in parallel were proposed[6]. In addition, a cage recombination mechanism was also invoked.

$$HO-[CH_2-CH(CH_3)-O]_x-CH(OOH)-CH(CH_3)-O-[CH_2-CH(CH_3)-O]_y H$$
$$\downarrow$$
$$HO-[CH_2-CH(CH_3)-O]_x-CH(O\cdot)-CH(CH_3)-O-[CH_2-CH(CH_3)-O]_y H$$
$$\downarrow$$
CAGE RECOMBINATION WITH HO·

$$\underset{\textbf{(K)}}{HO-[CH_2-CH(CH_3)-O]_x-C(O)-CH(CH_3)-O-[CH_2-CH(CH_3)-O]_y H} + H_2O$$

Pathway 1. C–C bond cleavage adjacent to the alkoxy centre takes place to generate product **E** and **L**.

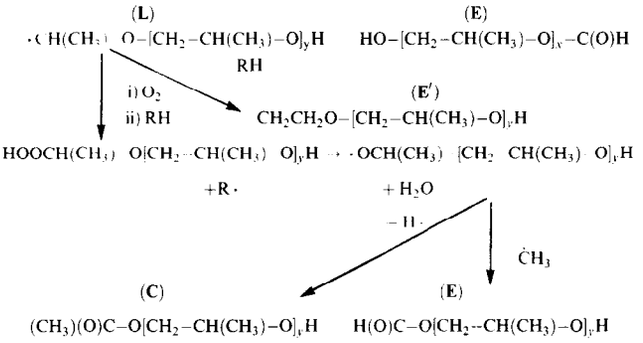

Pathway 2. C–O bond cleavage adjacent to the alkoxy group takes place to generate products **F'** and **M**.

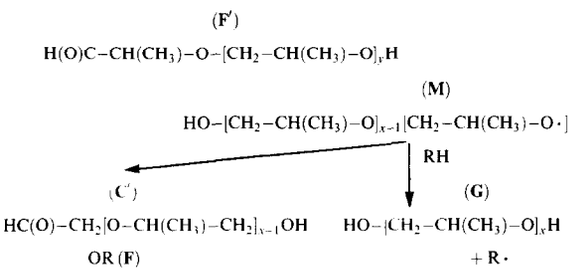

ESI

Electrospray spectra of untreated and pyrolysed (66 h/155°C) PPO at a cone voltage (*cv*) of 48 (*Figure 2*) show a distribution of singly-charged ions around 2000 Da, denoted as series A^+ and doubly-charged ions around 1000 Da, denoted as series A^{2+}. As expected, each species in series A^+ yields peaks at mass intervals of the monomer unit (58 Da) while series A^{2+} displays peaks at mass intervals of one-half the monomer unit (29 Da). All series show a well-defined ^{13}C isotopic splitting pattern (see inset to *Figure 2B*). As the *cv* is decreased, a greater concentration of doubly- and then triply-charged ions become apparent (data not shown). This effect is attributed to the variation in energy with *cv* of the collisions of multiply-charged solvated molecular ions in the cone-skimmer region and is well documented for PEGs[8] and proteins[9].

Fragmentation at high cv. At a *cv* greater than 30, an unexpected spread of ions below 600 Da is evident in the

pyrolysed *and* untreated samples. Selby *et al.*[10] suggest that protonation of polyglycols can occur at the oxygen atom during collision-induced dissociation (CID), followed by subsequent C–O bond cleavage to produce a shorter polyglycol chain and a secondary cation. We propose that the same process leads to the formation of these low-molecular-weight species at a *cv* greater than 30, thus

$$HO{-}[CH_2{-}CH(CH_3){-}O]_x{-}CH_2CH(CH_3){-}OH \cdot [CH_2{-}CH(CH_3){-}O]_yH$$

$$HO{-}[CH_2{-}CH(CH_3){-}O]_x{-}CH_2{-}\dot{C}H(CH_3) + HO{-}[CH_2{-}CH(CH_3){-}O]_yH$$

(H) (I)

$RMM = 1 + (58n)$ $RMM = 18 + (58n)$

Series I also exhibits H^+ (series J) adducts for $y = 6$ to $y = 11$. When x or $y = 5$ or less, only H^+ adducts are detectable, similarly, for x or $y = 12$ and above, only NH_4^+ adducts are detectable. This is due to the relative stability of the two ions at the *cv* employed, the H^+ adduct presumably being formed by the removal of NH_3 from the NH_4^+ adduct.

Table 2 shows the peak assignments for series A^+, A^{2+}, C/C′, E/E′, F/F′, G, H, I, J and K. In all cases except for series H and J, the entire series is not shown for the sake of brevity.

The thermal degradation products

Clearly the degradation of PPO has resulted in the development of a far more complex spectrum due to the production of degraded molecules: compare, for example, the region of series A^{2+} in *Figure 2A* with the region of series A^{2+} in *Figure 2B*.

Series K can only be attributed to oxidation at the secondary carbon atom, whereas all the other species (series C/C′, E/E′, F/F and G) can arise from oxidation at either the secondary or tertiary carbon atoms. Moreover the relatively high abundance of the ions due to series E suggests that oxidation at the secondary carbon atom predominates, as three separate pathways exist for the formation of series E (and E′) via the secondary oxidation mechanism.

Series I generated by *in situ* fragmentation and series G generated by thermal degradation coincide exactly with each other, and with series A^+, and are therefore not easily identifiable when $m/z > 1400$ Da as much unaltered PPO still remains. At lower mass, series I and G are however easily recognizable. The g.p.c. spectra display a lower concentration of low-mass (>1400 Da) degraded products than the ESI spectra. This, we believe, is in part due to the fragmentation occurring *in situ* during ESI analysis, producing in particular series I, thus emphasizing the concentration of thermally degraded products present at lower mass. The differing sensitivities of the two techniques also makes comparison difficult and may explain why the small concentration of higher mass material visible below 7.0 min elution time in the g.p.c. spectra is not visible in the ESI spectra. Calibration difficulties will obviously be encountered during the analysis of such a complex mixture. Very minor impurities may be responsible for skewing the molecular weight determination, even though the g.p.c. equipment has been calibrated with high purity standards[3].

MALDI

MALDI spectra of pyrolysed (66 h/155°C) and untreated PPO (*Figure 3*) were recorded at high and low laser power using sodium chloride to promote ionization. As with the ESI spectra, series A^+, C/C′, E/E′, F/F′ and G are easily recognizable. Multiply-charged ions are not, however, visible in the MALDI spectra.

The laser power was varied for every sample analysed. It was consistently found that increasing the laser power increased the concentration of degradation products appearing below ~1400 Da in the MALDI spectrum. This parallels the situation found with the ESI spectra where we suggest that *in situ* fragmentation occurs to produce series I at higher *cv*, thus emphasizing the concentration of thermal degradation products. Fragmentation of this type was seen only to a very minor extent in the untreated samples and only when the laser power was at a maximum. Creel[11] suggests that a loss of detector sensitivity may sometimes account for this phenomenon. Thus the microchannel plate array detector can be swamped by a large number of low-mass ions. If the detector does not recover sufficiently, the high-mass ions may be detected at a lower signal strength, resulting in a skewed mass distribution with concomitant mass average errors. This would explain the more variable mass distribution in the degraded samples, where a higher concentration of low-mass ions exists compared with the undegraded samples. Non-homogeneous mixing of the matrix and analyte could also produce similar mass discrepancies, as documented for poly(methyl methacrylate)[12]. Spectra run at lower laser power show good agreement with the polymer distribution pattern observed by g.p.c.

CONCLUSION

The degradation pathways involving C–C and C–O cleavage adjacent to the alkoxy radical centre suggested for PPO from ^{1}H n.m.r. measurements on the bulk material[6] were confirmed by characterization of all of the immediate products of decomposition, namely C/C′, E/E′, F/F′ and G, by ESI and MALDI experiments for each individual component of the PPO sample. However our results do point to a major (and possibly the major) role of the secondary alkoxy radical as compared with the tertiary alkoxy radical advocated by Griffiths *et al.*[6]. The mass spectrometric measurements also give an indication of the extent of pyrolysis. High cone voltages in ESI and high laser power in MALDI can lead to additional degradation of the PPO sample, but these can be avoided by using milder conditions.

ACKNOWLEDGEMENTS

Z.B. thanks the Defence Research Agency for a research studentship. EPSRC are thanked for a grant to purchase the electrospray equipment and for funding A.B. We thank Professor P.J. Derrick for access to the MALDI equipment. We also thank Professors G.G. Cameron, G. Camino and L. Costa for disclosure of preliminary results and for drawing our attention to the work of Lemaire *et al.*

REFERENCES

1 Nohmi, T. and Fenn, J. B. *J. Am. Chem. Soc.* 1992, **114**, 3241
2 Bahr, U., Andreas, D., Karas, M., Hillenkamp, F. and Giessmann, U. *Anal. Chem.* 1992, **64**, 2866
3 Compana, J. E., Sheng, L.-S., Shew, S. L. and Winger, B. E. *Trends Anal. Chem.* 1994, **13**, 239
4 Covey, T. R., Bonner, R. F., Shusan, B. I. and Henion, J. *Rapid Commun., Mass Spectrom.* 1988, **2**, 249
5 Smith, R. D., Loo, J. A., Edmonds, C. G., Baringa, C. J. and Udseth, H. R. *Anal. Chem.* 1990, **62**, 882
6 Griffiths, P. J., Hughes, J. H. and Park, G. S. *Eur. Polym. J.* 1993, **29**, 437
7 Lemaire, J. and Gauvin, P. *Makromol. Chem.* 1987, **188**, 1815
8 McEwen, C. N., Larsen, B. S. and Simonsick, W. J. *Abstracts 42nd ASMS Conference on Mass Spectrometry*, Chicago, 1994, 317
9 Loo, J. A., Udseth, H. R. and Smith, R. D. *Rapid Commun., Mass Spectrom.* 1988, **2**, 207
10 Selby, T. L., Wesdemiotis, C. and Lattimer, R. P. *J. Am. Soc. Mass Spectrom.* 1994, **5**, 1081
11 Creel, H. S. *TRIP* 1993, **1**, 1993
12 Corless, S., Tetler, L. W., Parr, V. and Wood, D. *Abstracts 42nd ASMS Conference on Mass Spectrometry*, Chicago, 1994